SEPARATING STRATEGIC CHOICE FROM FORECAST ERROR: ANALYTICAL AND SIMULATION INSIGHTS INTO DUTCH IMBALANCE PRICING

MATTIA ZEN
SNR:2132868

Supervisor: Reyer Gerlagh
Second Reader: Cedric Argenton

Tilburg School of Economics and Management
Tilburg University

June 17, 2025

Abstract

The increasing penetration of variable renewable energy (VRE) has increased forecast error, Area Control Error (ACE), and imbalance price volatility in European power systems. The policy debate has therefore focused on which tools can be effective in overcoming the issue. This thesis develops a closed-form analytical feedback model in which Transmission System Operator (TSO) reserve activation and Balancing Responsible Party (BRP) deviations interact recursively, explicitly separating intentional from stochastic imbalances. Parameterised with Dutch data and validated by Monte-Carlo simulation, the model yields three main results. (1) Once a stable feedback equilibrium exists, deterministic ACE components are fully neutralised; residual ACE equals the VRE shock under all the pricing rules evaluated. (2) Pricing design therefore affects only the distribution of balancing costs: end pricing shifts cost to the TSO leading to lower system cost, dual and conditional-dual shift it to BRPs. (3) Lower BRPs' adjustment cost allows them to absorb shocks cheaply and accurately without changing ACE variance. Therefore, according to this thesis, policy should prioritise improved VRE forecasting and targeted storage incentives; the decision of the settlement rule cannot decrease ACE.

Contents

List of Figures

Chapter 1

Introduction

Although variable renewable energy (VRE) generation, such as wind and solar, positively contributes to reducing greenhouse gas (GHG) emissions, it also poses serious challenges to power systems. Unpredictability in VRE production arises from the difficulty in correctly forecasting meteorological conditions, making it more challenging for VRE producers to form expectations on the level of electricity that can be generated (Acaroğlu and García Márquez, 2021; Goodarzi et al., 2019).

Electricity markets are structured to maintain grid stability by facilitating the trading of electricity among Balancing Responsible Parties (BRPs). BRPs are market entities responsible for forecasting, scheduling, and internally balancing their generation and consumption portfolios. This goal is achieved by trading energy in the day-ahead market, where participants submit bids for energy delivery the following day, and the intraday market, which allows adjustments closer to real-time delivery in response to updated forecasts (TenneT, 2022).

Despite these corrective layers, deviations between the scheduled and actual electricity flows inevitably arise due to stochastic demand and operational contingencies. Due to this issue, it is becoming complex for market regulators to maintain a real-time balance between power demand and supply.

In Continental Europe, an imbalance between supply and demand is measured at regional level (called an Area, such as the Netherlands) and quantified by the Area Control Error (ACE). ACE captures the difference between the forecasted and actual generation and consumption. ACE indicators include deviations in voltage (higher voltage when supply exceeds demand, lower voltage when demand exceeds supply) or unexpected cross-border power flows. Maintaining ACE close to zero ensures that the grid frequency remains constant at 50 Hz, as mandated by the EU regulation 2017/1485 of 23 November 2017 (Commission, 2017a,b).

To achieve this goal, national Transmission System Operators (TSOs, market regulators), whose mandate is to maintain grid balance and system frequency, instruct Balancing Service Providers (BSPs), prequalified entities capable of delivering upward or downward reserves, to activate additional capacity to respond to ACE deviation. This action aims to maintain a stable grid in their local area and target frequency at the European level

(TenneT, 2022).

Above, we described the 'active balancing market': the BSPs are actively instructed by the TSO to activate their reserves up or down. Complementary to this, the Netherlands has a passive balancing market. The passive balancing market operates through settlements after the closure of each 15-minute interval, so-called Imbalance Settlement Periods (ISPs), without any intervention by the TSO within these intervals. BRPs are instructed to pay for imbalances between their planned and actual generation or to receive compensation if they help reduce imbalances. This mechanism provides an incentive to help correct the system's deviations. The passive market operates as follows: Ex post, the TSO calculates the overall imbalance of individual BRPs over an entire ISP and the settlement price at which imbalances for all BRPs are valued.

Across Europe, different TSOs have implemented different settlement pricing mechanisms. As identified by van der Veen et al. (2010), the predominant pricing mechanisms are single pricing, where the same price is applied for positive and negative imbalances, and dual pricing, which sets different prices for upward and downward regulations. The Dutch TSO, TenneT, uses single pricing unless regulation state 2 occurs; in such cases, dual pricing is implemented.

The occurrence of regulation state 2 is considered an indicator of undesirable BSP activation swings. This regulation state is the label used for ISPs characterised by both upward and downward capacity activation, which are also non-monotonic. In other words, both up and down imbalances occur within the same ISPs, with no clear direction of the swing from one to the other. The appearance of regulation state 2 signals a drastic increase in operational balancing challenges for the TSO, as it requires more frequent and complex interventions.

Increased unpredictability in energy generation, particularly from VRE, leads to higher capacity activation volatility by BSPs and exacerbates price volatility in imbalance settlement prices. As a result, BRPs face greater financial risks when deviations from their schedules are observed. These increased risks are ultimately passed on to the final electricity consumers through higher imbalance costs. Although consumers do not observe an explicit charge for imbalance costs on their bills, these costs enter the calculation of wholesale and retail tariffs. Electricity suppliers adjust their pricing structures to account for the increased financial risks and higher imbalance settlement costs they face, thereby transferring these costs, indirectly, to end-users via higher energy prices. Therefore, it is crucial to identify pricing mechanisms that mitigate these risks for BRPs and incentivise them to reduce imbalances, thereby minimising costs for BSPs and reducing the financial burden on consumers.

Despite the importance of this matter, the literature does not agree on which system incurs the lowest cost. Wu et al. (2020) argue that while single pricing reduces imbalance costs, it fails to incentivise BRPs to minimise their imbalances, suggesting that dual pricing would be more effective in reducing system imbalance. However, van der Veen et al. (2010) found that single pricing encourages BRPs to maintain long positions, potentially leading to market inefficiencies, whereas dual pricing incentivises BRPs to balance their positions, even at the cost of higher imbalances. Koch (2021); Koch and Maskosa (2019) further emphasise that single pricing offers no distinction between BRPs

that help or harm the system, while dual pricing better aligns incentives for BRPs to mitigate imbalances, potentially encouraging more participation in the intraday market.

Furthermore, prior analyses lack an explicit, analytical separation between intentional and stochastic deviations, and neglecting the recursive interaction between BRP decisions and TSO interventions.

This thesis specifically addresses this analytical gap by developing a simplified closed-form model for the Dutch imbalance market, and explicitly distinguishes between intentional deviations (strategic actions by BRPs) and unintentional deviations (stochastic shocks) under different pricing mechanisms.

Specifically, it derives analytical solutions for the BRP and TSO policy functions under immediate and average pricing mechanisms. For more complex rules where closed-form solutions are not tractable, the analysis relies on numerical simulation to characterize market dynamics and outcomes. This combination of analytical and simulation-based methods allows for rigorous comparative statistics and policy analysis across different pricing designs.

Motivated by the ongoing debate in the literature and the practical challenges posed by increasing VRE penetration, this thesis addresses the following research questions:

- Which passive-market pricing mechanism (immediate, average, end, dual, conditional dual) yields
  - the lowest equilibrium ACE,
  - the lowest expected reserve-activation cost for the TSO,
  - the lowest expected imbalance-penalty cost for BRPs, and
  - the lowest combined system cost (TSO + BRPs)?
- How does pricing mechanisms shift the costs of balancing between the BSPs and BRPs?
- Can batteries play a crucial role in decreasing the system imbalance?

The scope of this analysis excludes complexities like cross-border trade and assumes homogeneity among BRPs for analytical tractability, limitations discussed comprehensively in Section 5.

Preliminary findings indicate that while different pricing rules substantially influence the distribution of balancing responsibilities and associated costs, they cannot fundamentally eliminate imbalances arising from unpredictable shocks, a significant insight given current policy emphasis.

The remainder of this thesis is structured as follows: Section 2 reviews pertinent literature, Section 3 introduces the analytical model and methodology, Section 4 discusses analytical and numerical results, Section 5 evaluates policy implications, limitations, and potential extensions, and Section 6 concludes.

Chapter 2

Literature Review

2.1 General Introduction on the Imbalance Market

In Europe, electricity trading occurs in day-ahead and intraday markets; however, real-time deviations between scheduled and actual flows still arise due to forecast errors and operational contingencies (TenneT, 2022). These discrepancies have grown with increasing VRE penetration, which exacerbates forecasting complexity and has drawn extensive research attention (Acaroğlu and García Márquez, 2021; Goodarzi et al., 2019). To correct these imbalances, TSOs instruct BSPs to activate reserves and restore system balance (TenneT, 2022; Yamujala et al., 2023). Imbalance settlement occurs over the ISP, during which TSOs calculate each BRP's net deviation and apply ex-post imbalance prices based on marginal reserve costs to penalise or reward deviations (Poplavskaya et al., 2020). This structure makes BRPs financially accountable for any deviation, directly linking their scheduling decisions to imbalance prices and motivating strategic behaviour in the face of uncertainty.

2.2 Consequences of VRE sources Incorporation in the energy mix

The literature agrees that the increase in the share of VRE sources in the energy mix played a crucial role in the recent increase in balancing price volatility.

Kazmi and Tao (2022) showed that, across 16 European systems, TSO's wind forecast errors have doubled, while solar forecast errors have increased fivefold over the past decade. The authors highlighted how these forecasting errors increase linearly with renewable generation, establishing a correlation between VRE penetration and the rise of this trend.

This view is supported by Miettinen and Holttinen (2019), who corroborated these findings at the regional level. The study showed that increasing the wind power share from 4% to 30% in the Nordic region nearly doubled the regional imbalance volumes.

The study highlights how this value changes drastically for different geographic locations: Finland's imbalance volume increased almost twice as much as that of other Nordic Countries.

In contrast, Miettinen et al. (2014) found that aggregating larger geographic areas (e.g. pooling multiple national grids) reduces forecast error. These results imply that stronger interconnections and market integration can mitigate, but not eliminate, VRE-driven imbalances.

In Germany, Hirth and Ziegenhagen (2013) observed the opposite trend. Despite a doubling of VRE capacity in the country, balancing reserve volumes fell by 20%. However, the authors attributed this unexpected result to enhanced cross-border and national cooperation and market reforms. These strong fluctuations in the imbalance volume affect the settlement price formation.

Obersteiner et al. (2010) identified different parameters driving imbalance costs in Austria, Denmark, and Poland. This study finds that the cost of imperfect forecasts, which is associated with forecasting errors, plays a crucial role in determining the imbalance price. Herrera de Silva and Horta (2018) reached similar conclusion evaluating the impact of VRE sources in the Iberian energy market between 2010 and 2015. The study found that VRE sources, especially wind, increased price volatility. The higher impact of wind energy over solar energy has been confirmed by Goodarzi et al. (2019) in the German market. The study also analysed the impact of these forecasting errors on the spot price[1], finding a larger impact of wind energy than that of solar energy in this analysis.

Together, these findings underscore that as the share of VRE increases, forecast-related imbalances and price volatility rise. This calls for improvements in forecasting and market integration. For example, Pierro et al. (2022) evaluated the Italian imbalance market and found that improving solar forecasts and national system connectivity can decrease solar energy variability by up to 60%.

2.3 Role of Batteries in the Imbalance Market

Battery Energy Storage Systems (BESS) have recently emerged as key systems for mitigating imbalances and reducing price volatility in electricity markets.

Padmanabhan et al. (2019) quantify the economic benefits, demonstrating that BESS can maximise social welfare by lowering the system's operational cost function and reducing the cost of activating reserves. Their analytical model showed that BESS can reduce price volatility by up to 44% during peak demand hours. This result is achieved because the BESS power stabilises prices in the long run. Jaffal et al. (2024) confirms these findings, showing that BESS delivers disproportionately larger benefits during peak-hour stress periods, effectively dampening extreme price swings when net demand spikes.

[1]Spot price refers to the price at which energy is traded in the day-ahead market.

A German case study by Angenendt et al. (2020) provides additional evidence at the national level: integrating photovoltaic-coupled BESS in German grids stabilises the system and reduces imbalance price volatility. This impact is estimated to lower the annual energy costs for the final consumer by 14.5%. Finally, Smets et al. (2023) reported that BESS deployment successfully reduced system imbalance in 75% of the events analysed, underscoring BESS's consistent ability to absorb unexpected surplus or supply deficits on short notice.

Together, these studies highlight the critical role of BESS in enhancing real-time balancing, particularly under high VRE penetration, by providing rapid bidirectional flexibility that both TSOs and BRPs can leverage to maintain grid stability and contain imbalance costs.

2.4 European Imbalance Energy Market

2.4.1 European Regulatory Framework

The European imbalance energy market, guided by the Electricity Balancing Guideline (EB GL), aims to harmonise balancing energy procurement and settlement across Europe, enhancing economic and technical efficiency while ensuring system security. The EB GL proposes different measures to improve system efficiency, starting from the IGCC platform, facilitating imbalance netting to avoid simultaneous opposite capacity activations (ENTSO-E, 2016). Moreover, platforms like TERRE and MARI coordinate the activation of replacement reserves and manual Frequency Restoration Reserves (mFRR) across borders (ENTSO-E, a, 2017).

In addition, the PICASSO platform integrates European automatic Frequency Restoration Reserves (aFRR). The platform enhances economic and technical efficiency by optimising the allocation of bids across neighbouring countries (ENTSO-E, b). Backer et al. (2023), compared the introduction of this platform to the existing IGCC framework, finding that PICASSO would lead to an estimated annual economic surplus of approximately 400 million EUR for the participating countries.

2.4.2 Cross-border Cooperation

Pooling reserves across borders has proven to be one of the most effective ways to cut costs and improve overall stability, leading to significant efficiency gain in the European market. Roumkos et al. (2022) show that, when Austria and Germany began sharing balancing energy more extensively, both countries saw noticeable drops in balancing activated capacity and energy prices. Earlier, van der Veen et al. (2011) calculated that trading balancing energy across borders could slash total imbalance costs by 40–50%, primarily due to the import of balancing energy from countries with cheaper generating resources. Topler and Polajzer (2020) expand on this in a dynamic simulation, finding that simply optimising how and when cross-border reserves are activated leads to substantial cost savings. Taken together, these studies make a strong case that regional

cooperation is critical, especially as VRE penetration increases and local imbalances become harder to manage in isolation.

2.4.3 Imbalance Pricing Mechanisms in Europe

Researchers have looked closely at how different imbalance pricing rules shape BRPs behaviour and market efficiency, and there is still no consensus on which mechanism yields the lowest system costs. In Finland, Helander et al. (2010) compare the Finnish, Danish and Swedish pricing mechanism, based on a two-price system[2], with Norway, which adopt a one-price system[3].

They find that dual pricing initially drives higher imbalance costs, but as wind's share grows, that difference shrinks, suggesting that single pricing's relative advantage on cost difference fades in very high-VRE systems.

Haring et al. (2015) propose a new "incentive-compatible" imbalance procedure to address the fact that many current schemes fail to properly reward BRPs who actively help rebalance the grid. This new mechanism takes into account not only the reserve capacity, but also the deployed energy[4] in a non-linear pricing scheme. By ensuring BRP actions align with system stability, their method tries to overcome the limitations of both single and dual pricing.

On a more quantitative front, Shinde et al. (2021) build a Mixed Integer Linear Program (MILP) to test various market scenarios under heavy VRE production. The authors evaluated a single pricing mechanism, where the imbalance price is settled based on the marginal cost of the net imbalance volume during the ISP, a dual pricing, where different price for up and down regulation are considered dividing total cost of down (up) bid for the total volume of down (up) regulated capacity, and a single pricing with spot reversion. They identified the single pricing mechanisms as the more market efficient, resulting in higher saving for the TSO and easier forecasting for the BRPs. This is achieved thanks to the marginal cost scheme compared to the average one used in the dual pricing. In contrast, Wu et al. (2020), analysed the pricing mechanisms adopted in eight Chinese regions and argue that, although single pricing keeps imbalance costs lower overall, it does not give BRPs the right incentives to shrink their deviations; dual pricing, they state, better encourages BRPs to balance their positions, even if it means slightly higher imbalance costs.

van der Veen et al. (2010) echoes this trade-off in his broader survey of six pricing mechanisms: single pricing tends to push BRPs into long positions. This result is

[2]The above-mentioned countries two-price system is designed as follow: the BRPs that increase the overall market imbalance pays the maximum or minimum of the prices during the ISP, while the regulation price for BRPs that help the system will be paid according to the spot price. An additional fixed volume price is added for both prices.

[3]Norway single pricing is designed as follow: the regulation price for all the BRPs is based on the marginal regulation price in the main regulation direction, regardless of the of the BRP's imbalance direction.

[4]The deployed energy refers to the real-time deliver of energy by the BSPs, while the reserve capacity is the agreement to provide energy signed between the BSPs and the TSO.

achieved showing that the BRPs profit for a long position is higher than for short positions. The higher profit is attributed to a lower cost for downward regulation compared to upward ones. On the other hand, the authors claim that dual pricing nudges the BRPs toward balance, albeit at the expense of somewhat higher imbalance-settlement fees.

Finally, Koch (2021) points out a basic flaw in many single-price systems: BRPs that help the system and those that hinder it both receive, or pay, the same rate, reducing the incentive to correct imbalances. The authors attribute this result mainly to the asymmetric spread between intraday and imbalance price: even if the probability of the system being short is above 0.5, it can be more rewarding for the BRPs to take short position to stress the system. Koch and Maskosa (2019) confirm this in the German market: they empirically showed a shift toward system shortage and that, when the system is short, the spread between the intraday and the imbalance price is smaller, revealing an asymmetry in the pricing incentives.

All these findings underline just how sensitive BRP behaviour is to pricing design, and why a detailed comparison of these mechanisms is crucial for any system grappling with rising VRE uncertainty.

2.5 Methodology Used

2.5.1 Agent-Based Modelling

Agent-Based Modelling (ABM) has been widely used in the literature to study balancing markets (Poplavskaya et al., 2020; Roben and de Haan, 2019; van der Veen et al., 2011). ABMs simulate the decentralised interactions of heterogeneous agents, such as BRPs, and allow emergent system-level dynamics to be analysed (Weidlich and Veit, 2008).

In particular, van der Veen et al. (2011) used this framework to explore how different balancing market designs, including various pricing mechanisms, affect BRP behaviour. His work highlights the critical role of pricing rules in shaping BRPs' behaviour and overall market efficiency.

2.5.2 Other Common Methodologies Adopted

While ABMs are widely used in the balancing market literature to capture heterogeneity and adaptive learning (Poplavskaya et al., 2020; Roben and de Haan, 2019; van der Veen et al., 2011), other modelling approaches were also applied.

Game-theoretical models have been used to analyse the strategic interactions among rational agents (Ehrhart and Ocker, 2021). The model focuses on how market participants anticipate and respond to each other's actions using the dependency between wholesale and balancing markets. These models are well-suited for auction design and equilibrium analysis but typically require strong assumptions on strategic behaviour and market structure.

Secondly, Just and Weber (2008) solve the market interaction with numerical simulation models relying on algorithmic procedures. These models are useful for incorporating detailed system constraints but often sacrifice interpretability and closed-form insight.

Despite the diversity of approaches, none of these offer an analytical solution that explicitly models both the intentional and unintentional imbalances of BRPs under different pricing mechanisms. This thesis contributes to the literature by developing such an analytical framework, offering strong insights into the closed-form feedback loop between BRPs and TSO. The analytical results are then validated using a numerical simulation model.

2.6 Summary of the Literature

The existing literature demonstrates that rising VRE penetration has amplified forecast errors, imbalance volumes, and price volatility, despite partial mitigation through cross-border cooperation and storage (Angenendt et al., 2020; Goodarzi et al., 2019; Kazmi and Tao, 2022; Topler and Polajzer, 2020). Yet the literature does not agree on the pricing rules that better overcome this issue (Backer et al., 2023; Roumkos et al., 2022). Recent studies highlight a trade-off: single pricing lowers BRPs costs but weakens their incentives to correct the deviation, while dual pricing strengthens these incentives at the expense of higher imbalance cost. These studies rely primarily on simulations or empirical observations without isolating intentional from stochastic imbalances (Shinde et al., 2021; van der Veen et al., 2010; Wu et al., 2020).

In summary, there is no analytical framework within the literature that (1) separates intentional BRP deviations from VRE-driven shocks, (2) models their recursive interaction with TSO reserve activation, and (3) compares pricing rules in closed form. The next chapter introduces such a model, filling this gap by providing transparent, quantitative insight into how pricing design influences BRP behaviour and system efficiency under high VRE uncertainty.

Chapter 3

Methodology

3.1 Description of the Model

The model is developed in two complementary stages. First, I develop a simplified analytical model in which BRPs and the TSO follow linear feedback rules, determined by β_i and α_i respectively, under the existence of unintentional shock. I derive closed-form expressions for these feedback gains under two pricing mechanisms, immediate and average pricing.

Second, I implement a simulation in Python, calibrating the parameters with realistic values. The goal of the simulation is to verify the analytical results, explore parameter sensitivity, and compare equilibrium statistics (ACE, BRP costs, price volatility) across pricing rules.

3.1.1 Variables

Time In the Dutch market, an ISP, denoted by T, has a duration of 15 minutes. We divide each ISP into two sub-periods of 7.5 minutes: $t \in T = \{1, 2\}$. Let L refer to the previous ISP, so $L2$ denotes the second sub-period of the previous ISP. Crucially, BRPs do not observe real-time activation. TenneT publishes activated capacity with a delay: approximately 5 minutes from 3 December 2024. Hence, in our model, at the beginning of sub-period t, each BRP only observes capacity activated in the immediately preceding sub-period $t - 1$.

BRP Imbalance The net position of BRPs in real-time is composed of intentional and unintentional deviations:

$$I_{i,t} = x_{i,t} + \mu_{i,t} \tag{3.1}$$

Here, subscript i denotes the individual BRP, and t the time period. When the index i is omitted, the variable refers to the aggregate across all BRPs.

Each BRP adopts a linear decision rule for intentional deviations, based on the previously activated capacity by BSPs as ordered by the TSO:

$$x_{i,1} = \beta_1 c_{L2} + \beta_3 c_{L1} \tag{3.2}$$

$$x_{i,2} = \beta_2 c_1 + \beta_4 c_{L2} \tag{3.3}$$

The parameters $\beta_1, \beta_2, \beta_3, \beta_4$ represent "feedback gains", indicating the sensitivity of BRPs' intentional deviations x_t to past BSP activations. In the thesis, we refer to these as the "betas".

For tractability, we assume the BRP's decision rule follows a linear structure, enabling us to derive closed-form solutions for α and β, clarifying how BRPs and the TSO respond to recent activation signals.

We assume unintentional deviations to follow a first-order autoregressive process, AR(1):

$$\mu_t = \rho \mu_{t-1} + \epsilon_t, \quad \epsilon_t \sim \mathcal{N}(0, \sigma^2), \tag{3.4}$$

Where $0 < \rho < 1$ is the correlation of the unintentional deviation over time and ϵ_t is the unpredictable component.

TSO Capacity The TSO instructs BSPs to activate capacity to balance supply and demand in real time. Given the hierarchical structure (TSO commanding BSPs), we model the TSO and BSPs as a single entity.

The TSO chooses c_t to minimize Area Control Error (ACE), defined as the sum of intentional and unintentional deviation and BSP's capacity activated:

$$A_t = x_t + \mu_t + c_t \tag{3.5}$$

We assume the TSO targets to keep the ACE close to zero, or practically, the minimisation of the quadratic function of the ACE. Using a square loss function instead of absolute values to set ACE close to zero, allows us to solve the model analytically, and it weighs more the extreme values.

$$\min_{c_t} A_t^2 = (x_t + \mu_t + c_t)^2 \tag{3.6}$$

Given the information available for the TSO , we assume the policy function for the capacity activation to depend on the previous level of ACE , and the previous two levels of activated capacity. The coefficient ρ captures the persistence of the unintentional deviation, reflecting the fraction of ACE that is forecastable due to the AR(1) process.

$$c_1 = -\rho A_{L2} + \alpha_1 c_{L2} + \alpha_3 c_{L1} \tag{3.7}$$

$$c_2 = -\rho A_1 + \alpha_2 c_1 + \alpha_4 c_{L2} \tag{3.8}$$

The parameters $\alpha_1, \alpha_2, \alpha_3, \alpha_4$ capture the TSO's feedback gains, showing how activated capacity c_t responds to past signals when minimizing expected squared ACE.

3.1.2 Assumptions

Linear Marginal Cost of Balancing for the TSO

We assume that the TSO's marginal cost of procuring balancing energy is linear in the amount of capacity it activates. The subperiod price reflects the marginal cost of balancing:

$$p_t(c_t) = \gamma c_t, \quad \gamma > 0 \tag{3.9}$$

This assumption determines the sub-period price p_t, which is the cost of activating additional upward or downward reserves. In our model, we assume the cost to be symmetric for both upward and downward adjustments.

Linear Marginal Cost of Balancing for Intentional Deviation

We model each BRP's intentional deviation $x_{i,t}$ with a quadratic cost function:

$$C_{i,t} = \frac{1}{2}\theta(x_{i,t})^2 \quad \Rightarrow \quad MC_{i,t} = \theta x_{i,t}, \quad \theta > 0 \tag{3.10}$$

When BRPs set their intentional deviation, they incur a cost for reducing or increasing generation. We assume this cost is symmetric for both upward and downward adjustments.

Atomic BRPs

We model a representative BRP as atomic: its individual intentional deviation $x_{i,t}$ is infinitesimal relative to aggregate system volume. Thus, it cannot influence the equilibrium imbalance price p_T. Formally, the BRP takes the price as exogenous and solves:

$$\max_{x_{i,t}} \ \mathbb{E}\left[p_T I_{i,t} - \frac{1}{2}\theta(x_{i,t})^2\right] \tag{3.11}$$

This price-taking assumption prevents a single large BRP from stressing the system and manipulating the imbalance price. Dropping this assumption implies that a specific BRP could influence the system imbalance and, in turn, alter the equilibrium price, thus changing the nature of the optimisation problem.

3.1.3 Parameters and Variables

Table 3.1: Model Parameters, Interpretation and Domains

Parameters	Meaning	Domain
$\alpha_1, \alpha_2, \alpha_3, \alpha_4$	TSO feedback parameters: These coefficients determine the TSO's response to past capacities in adjusting future capacity.	$\alpha_1, \alpha_2, \alpha_3, \alpha_4 \in \mathbb{R}$
$\beta_1, \beta_2, \beta_3, \beta_4$	BRP feedback parameters: These coefficients capture how strongly a BRP's intentional deviation $x_{i,t}$ responds to past capacities and imbalances.	$\beta_1, \beta_2, \beta_3, \beta_4 \in \mathbb{R}$
γ	Price coefficient: Determines the cost of activating capacity for the BSPs.	$\gamma > 0$
θ	Adjustment cost parameter: Controls the cost of the BRP's intentional deviation; reflects penalty per unit of deviation.	$\theta > 0$
ϵ	Random unintentional shock.	$\epsilon \sim \mathcal{N}(0, \sigma_\epsilon^2)$
σ_ϵ	Standard deviation (SD) of the unintentional shock.	$\sigma_\epsilon \in \mathbb{R}_+$
ρ	Persistence of the unintentional imbalance: autoregressive parameter influencing current imbalance via the past.	$0 \leq \rho \leq 1$
$x_{i,t}$	Intentional deviation of a representative BRP in subperiod t.	$x_{i,t} \in \mathbb{R}$
$\mu_{i,t}$	Unintentional deviation (stochastic shock) of a representative BRP in subperiod t.	$\mu_{i,t} \in \mathbb{R}$
A_t	ACE at the end of subperiod t.	$A_t \in \mathbb{R}$
p_t	Price for subperiod t.	$p_t \in \mathbb{R}$
p_T	Settlement price for the current ISP.	$p_T \in \mathbb{R}$

3.1.4 Equilibrium Condition

Recalling from Equation 3.5, the TSO aims to minimise the expected ACE in the current period. To do this, it forms expectations on the level of intentional and unintentional deviations by BRPs at the start of each time period:

$$c_1 = -\mathbb{E}_1[x_1 + \mu_1] \tag{3.12}$$
$$c_2 = -\mathbb{E}_2[x_2 + \mu_2] \tag{3.13}$$

At the same time, each BRP chooses its intentional deviation to maximise profit according to the pricing rule (refer to Equation 3.11):

$$\theta x_{i,1} = \mathbb{E}_1[p_T] \tag{3.14}$$
$$\theta x_{i,2} = \mathbb{E}_2[p_T] \tag{3.15}$$

The computation of p_T depends on the pricing mechanism in use, as described below.

3.1.5 Pricing Mechanisms

We analyse five distinct pricing mechanisms: immediate, average, and, dual, and conditional dual pricing.

Immediate Pricing. The imbalance price is equal to the subperiod price in t, and depends only on current capacity:

$$p_T = p_t = \gamma c_t \tag{3.16}$$

This mechanism departs from how imbalance prices are determined in real world scenario, where pricing is based on aggregate capacity over the full ISP. Since European data are recorded per ISP, the implementation of this pricing mechanism is not feasible. However, it is analysed here to provide a simplified version of the model and a benchmark for subsequent analysis since, intuitivelly, is the ideal pricing mechanism to decrease system cost, without arbitrage opportunities.

Average Pricing. The settlement price is the arithmetic average of the two subperiod prices:

$$p_T = \frac{p_1 + p_2}{2} = \gamma \cdot \frac{c_1 + c_2}{2} \tag{3.17}$$

End Pricing. The price depends solely on the final subperiod:

$$p_T = p_2 = \gamma c_2 \tag{3.18}$$

Dual Pricing. The price is determined by the maximum price or the ISP if the BRP deviation is above 0, the minimum price otherwise:

$$p_T = \begin{cases} \max(p_1, p_2) & \text{if } I_{i,1} + I_{i,2} > 0 \\ \min(p_1, p_2) & \text{if } I_{i,1} + I_{i,2} \leq 0 \end{cases} \tag{3.19}$$

Conditional Dual Pricing. The price depends on direction of activated capacity in $t = 1$ and $t = 2$. If c_1 and c_2 have the same sign, the price is the $\max(p_1, p_2)$ for positive and $\min(p_1, p_2)$ for negative.

In the case of activation of both upward and downward capacity, meaning that they have opposite sign, the price depends on the individual BRP's net deviation, $I_(i, 1) + I_(i, 2)$. The minimum subperiod price is applied when the net deviation is positive, the maximum when negative.

This pricing mechanism is the most similar to the Dutch system.

$$p_T = \begin{cases} \max(p_1, p_2) & \text{if } c_1; c_2 > 0 \\ \min(p_1, p_2) & \text{if } c_1; c_2 < 0 \\ \max(p_1, p_2) & \text{if } c_1 c_2 < 0 \text{ and } I_{i,1} + I_{i,2} < 0 \\ \min(p_1, p_2) & \text{if } c_1 c_2 < 0 \text{ and } I_{i,1} + I_{i,2} \geq 0 \end{cases} \tag{3.20}$$

3.2 Analytical Solution

Solving the model for $t = 1$ requires substituting the parametric Equation 3.2 and 3.7 and the AR(1) process (Equation 3.4) into the equilibrium conditions (Equation 3.12 and 3.14). In Equation 3.14 the imbalance price p_T is determined by different pricing mechanisms. This thesis solves the model analytically under the immediate and average pricing rules and use the closed-form results to validate the simulation outcomes.

3.2.1 Immediate Pricing

Plugging the equation for the ACE (Equation 3.5) into the equation for the AR(1) process (Equation 3.4) we have:

$$\mathbb{E}_1[\mu_1] = \rho\mu_{L2} = \rho(A_{L2} - c_{L2} - x_{L2}) \tag{3.21}$$

Where the value of x_{L2} is not known, thus we plug in Equation 3.3 into Equation 3.21:

$$\mathbb{E}_1[\mu_1] = \rho(A_{L2} - c_{L2} - \beta_2 c_{L1} - \beta_4 c_{LL2}) \tag{3.22}$$

We neglect the third- and higher-order lags, meaning that we remove the expectation formed in $t = 1$ based on c_{LL2}, and in $t = 2$ based on c_{L1}. We do this because of the diminishing impact of deeper lags and for analytical tractability since adding a third lag in the analysis becomes extremely unwieldy. Since the first two lags capture the bulk of the predicable variance, we expect a small change in the results. This generalisation allows us to write the expectation of unintentional imbalance as:

$$\mathbb{E}_1[\mu_1] = \rho\mu_{L2} = \rho A_{L2} - \rho c_{L2} - \rho\beta_2 c_{L1} \tag{3.23}$$

Which is the expectation formed in $t = 1$ on the value of unintentional deviation.

Similarly, the TSO forms expectations on the value of intentional deviation according to the policy function (Equation 3.2)

$$\mathbb{E}_1[x_1] = \beta_1 c_{L2} + \beta_3 c_{L1} \tag{3.24}$$

Plugging in Equation 3.23 and 3.24 into the equilibrium condition Equation 3.12, we find the value of activated capacity in t=1:

$$c_1 = -\mathbb{E}_1[x_1 + \mu_1] = -\rho A_{L2} + (\rho - \beta_1)c_{L2} + (\rho\beta_2 - \beta_3)c_{L1} \tag{3.25}$$

Similarly for t=2:

$$c_2 = -\mathbb{E}_2[x_2 + \mu_2] = -\rho A_1 + (\rho - \beta_2)c_1 + (\rho\beta_1 - \beta_4)c_{L2} \tag{3.26}$$

At the same time the BRP sets its level of intentional deviation to maximise its profit as described in Equation 3.11. Plugging in the parametric equation for the value of activated capacity Equation 3.7 we have:

$$\theta x_1 = \gamma \mathbb{E}_1[c_1] \Rightarrow x_1 = \frac{\gamma}{\theta}(\alpha_1 c_{L2} + \alpha_3 c_{L1}) \tag{3.27}$$

This is because the BRP believes the BSP will successfully set expected ACE to zero, $\mathbb{E}_t[A_{t-1}] = 0$ following Equation 3.6.

Similarly for t=2:

$$x_2 = \frac{\gamma}{\theta}(\alpha_2 c_1 + \alpha_4 c_{L2}) \tag{3.28}$$

Resubstituting Equations 3.25, 3.26, 3.27, and 3.28 into the initial parametric equations we capture the feedback loop between BRP behaviour and TSO reaction.

To achieve it we substitute the values of x_t and c_t and compare the coefficients for c_1, c_{L2} and c_{L1}. After the comparison the feedback loop is explained by this set of equations:

$$\alpha_1 = \rho - \beta_1, \quad \beta_1 = \frac{\gamma}{\theta}\alpha_1 \tag{3.29}$$

$$\alpha_2 = \rho - \beta_2, \quad \beta_2 = \frac{\gamma}{\theta}\alpha_2 \tag{3.30}$$

$$\alpha_3 = \rho\beta_2 - \beta_3, \quad \beta_3 = \frac{\gamma}{\theta}\alpha_3 \tag{3.31}$$

$$\alpha_4 = \rho\beta_1 - \beta_4, \quad \beta_4 = \frac{\gamma}{\theta}\alpha_4 \tag{3.32}$$

The alphas reflect how the TSO's policy transmits those capacities into price signals, while the betas reflect how BRPs internally weigh past capacities in forming expectations. In equilibrium, each BRP sets its marginal revenue, proportional to the TSO's price coefficient γ, equal to its marginal adjustment cost θ, which gives $\beta = \frac{\gamma}{\theta}\alpha$. Intuitively, BRPs scale their response to capacity signals by the ratio of the price they can earn γ

to their own cost of intentional imbalance θ, even as the TSO itself adjusts capacity based on the ACE signal.

Solving the system of Equations 3.29, 3.30, 3.31, and 3.32 for α and β we find the solution of the model for immediate pricing as function of the parameters ρ, γ, and θ:

$$\alpha_1 = \alpha_2 = \frac{\rho\theta}{\theta + \gamma}, \quad \beta_1 = \beta_2 = \frac{\rho\gamma}{\theta + \gamma} \tag{3.33}$$

$$\alpha_3 = \alpha_4 = \left(\frac{\theta\gamma\rho}{\theta + \gamma}\right)^2, \quad \beta_3 = \beta_4 = \left(\frac{\rho\gamma}{\theta + \gamma}\right)^2 \tag{3.34}$$

Note that these expressions are conditional to $E_t[A_{t-1}] = 0$. If the BRPs deviate from the equilibrium policy rules described in Section 3.1.1, the assumptions no longer hold, and the feedback loop derived above is not optimal.

3.2.2 Average Pricing

The same process described in Section 3.2.1 is applied under the average pricing mechanism, where the settlement price is defined in Equation 3.17. In this case, the BRP's expectation on the price in $t = 1$ is based on the expected capacity activated in both $t = 1$ and $t = 2$, while the expectation in $t = 2$ depends on the realized value at $t = 1$ and the expected value at $t = 2$.

Substituting Equations 3.7 and 3.8 into 3.17 and 3.14 yields:

$$x_1 = \frac{\gamma}{\theta} \cdot \frac{\mathbb{E}_1[c_1] + \mathbb{E}_1[c_2]}{2} = \frac{\gamma}{2\theta} \left[c_{L2}(\alpha_1 + \alpha_1\alpha_2 + \alpha_4) + c_{L2}\alpha_3(1 + \alpha_2)\right] \tag{3.35}$$

$$x_2 = \frac{\gamma}{\theta} \cdot \frac{c_1 + \mathbb{E}_2[c_2]}{2} = \frac{\gamma}{2\theta} \left[c_1(1 + \alpha_2) + c_{L2}\alpha_4\right] \tag{3.36}$$

The TSO's decision rules remain as defined in Equations 3.25 and 3.26. Substituting the BRP policy into these yields the updated parametric relationships:

$$\alpha_1 = \rho - \beta_1, \quad \beta_1 = \frac{\gamma}{2\theta}(\alpha_1 + \alpha_1\alpha_2 + \alpha_4) \tag{3.37}$$

$$\alpha_2 = \rho - \beta_2, \quad \beta_2 = \frac{\gamma}{2\theta}(1 + \alpha_2) \tag{3.38}$$

$$\alpha_3 = \rho\beta_2 - \beta_3, \quad \beta_3 = \frac{\gamma}{2\theta}\alpha_3(1 + \alpha_2) \tag{3.39}$$

$$\alpha_4 = \rho\beta_1 - \beta_4, \quad \beta_4 = \frac{\gamma}{2\theta}\alpha_4 \tag{3.40}$$

This yields the following closed-form solutions:

$$\alpha_1 = \rho \cdot \frac{2\theta + 2\gamma - \gamma(1 + \rho)}{2\theta + 2\gamma}, \quad \beta_1 = \frac{\gamma\rho(1 + \rho)}{2\theta + 2\gamma} \tag{3.41}$$

$$\alpha_2 = \frac{2\theta\rho - \gamma}{2\theta + \gamma}, \quad \beta_2 = \frac{\gamma(1+\rho)}{2\theta + \gamma} \tag{3.42}$$

$$\alpha_3 = \frac{\rho\gamma(1+\rho)}{2\theta + 2\gamma + \rho\gamma}, \quad \beta_3 = \frac{\gamma^2\rho(1+\rho)^2}{(\gamma + 2\theta)(\gamma\rho + 2\gamma + 2\theta)} \tag{3.43}$$

$$\alpha_4 = \frac{\gamma\theta\rho^2(1+\rho)}{2\theta^2 + 3\theta\gamma + \gamma^2}, \quad \beta_4 = \frac{\gamma^2\rho^2(1+\rho)}{4\theta^2 + 6\theta\gamma + 2\gamma^2} \tag{3.44}$$

3.3 Simulation

Simulation both validates our analytical results for immediate and average pricing and extends the analysis to more complex pricing mechanisms, evaluating system cost, TSO and BRP expenses, price volatility, and ACE.

To explore the implications of different pricing mechanisms, I simulate the strategic interaction between BRPs and the TSO over 10,000 ISPs. The simulation iteratively solves the model by alternating the optimization of behavioural parameters α and β under different pricing rules. For each scenario, the evolution of imbalance, activated capacity, and system costs are tracked. Implementation details, including the class structure and calibration metrics, are reported in the Appendix 7.1.

3.3.1 Simulation Setup

The simulation was implemented in Python. The numerical computations rely on standard scientific libraries such as NumPy, Pandas, SciPy, and Matplotlib[1] respectively for numerical routines, data management, optimisation, and visualisation. The core simulation is based on a discrete-time stochastic model where unintentional deviations follow an AR(1) process. Reproducibility is ensured by fixing the random seed prior to generating stochastic shocks. The pricing mechanisms are compared across multiple iterations using numerical optimisation routines to estimate equilibrium parameters for each scenario.

Real Data Calibration of the Parameters

Model calibration is performed using TenneT imbalance data for the period September 2023–September 2024, prior to the integration of the Netherlands into the PICASSO platform. This structural change has increased the cross-border trade, while in our model we assumed it to be zero.

The four key parameters that are calibrated are: γ (costs of BSP activation), θ (costs of BRP intentional activation), ρ (autocorrelation of unintentional imbalance), and σ_ϵ (standard deviation for unintentional shocks).

[1]Link to the libraries used: NumPy: https://numpy.org/, Pandas: https://pandas.pydata.org/, SciPy: https://scipy.org/, Matplotlib: https://matplotlib.org/.

The calibration targets the conditional dual pricing regime, which is the closest one to the Dutch market's settlement rules. Parameters are iteratively adjusted to minimise the difference between simulated and observed statistics. Full calibration procedure, including precise update rules and code-specific implementation details, is documented in Appendix 7.2.

Table 3.2: Parameter Calibration Using Dutch Imbalance Data (Sept 2023–2024)

Parameter	**Value**	**Target**		**Simulation**	**Observed**
σ_ϵ	17.85	σ_c	Standard deviation for BSPs activated capacity, ISP aggregate	25.1	27.82 MW
ρ_μ	0.85	ρ_c	Correlation between BSP activation across subsequent ISPs	0.43	0.737
γ	9.05	σ_p	Standard deviation of imbalance settlement price	189.8	179.46 EUR/MW
θ	5.18	$\sigma_{x+\mu}$	Standard deviation for total BRP imbalance	43.4	61.27 MW

The autocorrelation of the BRP activation differs from the observed value because the calibration process clips ρ at 0.85 to avoid numerical overflow. When ρ approaches 1, the iterative update formulas produce excessively large intermediate values that exceed floating-point limits. As a result, both the autocorrelation and the standard deviation of total BRP imbalance fall below their empirical targets.

Chapter 4

Results

4.1 Analytical Results

4.1.1 Comparative Statistics

BRP Response We begin by comparing the first-period BRP responsiveness to c_{L2} (β_1) under immediate (Equation 3.33) and average pricing (Equation 3.41):

$$\beta_1^{\text{imm}} = \frac{\rho\gamma}{\theta+\gamma}, \quad \beta_1^{\text{avg}} = \frac{\gamma\rho(1+\rho)}{2(\theta+\gamma)} \tag{4.1}$$

Because $\frac{1+\rho}{2} < 1$ for $0 < \rho < 1$, it follows that:

$$\beta_1^{\text{imm}} > \beta_1^{\text{avg}} \tag{4.2}$$

Under immediate pricing, the imbalance price depends solely on c_1, so BRPs can accurately anticipate p_1 based on c_1 alone. Under average pricing, the price $p_T = \gamma \cdot \frac{c_1+c_2}{2}$ also depends on future capacity c_2, increasing price uncertainty and reducing the BRP's responsiveness in period 1.

When shocks are highly persistent ($\rho \to 1$), future capacity is strongly determined by current capacity, i.e., $c_1 \approx c_2$, and:

$$p_T = \gamma \cdot \frac{c_1 + c_2}{2} \Rightarrow p_T \approx \gamma c_t \tag{4.3}$$

In this limit, BRPs' first-period response under average pricing converges to that under immediate pricing.

Additionally, because c_1 becomes known at $t = 2$, BRPs can form a more accurate expectation of c_2, increasing their responsiveness. Hence, we expect:

$$\beta_2^{\text{avg}} > \beta_1^{\text{avg}} \tag{4.4}$$

Recalling Equations 3.42 and 3.41, this inequality is confirmed analytically. In other words, BRPs weight the most recent capacity signal more heavily in the second sub-period than in the first under average pricing.

TSO Response Since BRPs are less responsive in $t = 1$ under average pricing (Equation 4.2), we expect the TSO to counter-balance this lack of responsiveness and increase their reliance on c_{L2} to keep ACE near zero. Thus, we expect:

$$\alpha_1^{\text{imm}} < \alpha_1^{\text{avg}} \tag{4.5}$$

Analytically:

$$\frac{\theta\rho}{\theta+\gamma} < \frac{2\theta\rho + \rho\gamma - \gamma\rho^2}{2(\theta+\gamma)} \tag{4.6}$$

Which simplifies to:

$$\frac{\gamma\rho(\rho-2)}{2(\theta+\gamma)} < 0 \quad \text{for } 0 < \rho < 1 \tag{4.7}$$

The inequality confirms the intuition in Equation 4.5.

Conversely, because BRPs respond more in $t = 2$ under average pricing ($\beta_2^{\text{avg}} > \beta_2^{\text{imm}}$), we expect:

$$\alpha_2^{\text{imm}} > \alpha_2^{\text{avg}} \tag{4.8}$$

Analytically:

$$\frac{\rho\theta(2\theta+\gamma) - (2\theta\rho - \gamma)(\theta+\gamma)}{(2\theta+\gamma)(\theta+\gamma)} > 0 \tag{4.9}$$

Which simplifies to:

$$\frac{\gamma(\gamma + \theta(1-\rho))}{2\theta^2 + 3\theta\gamma + \gamma^2} > 0 \tag{4.10}$$

Thus, Equation 4.10 analytically supports our intuition that TSO's reliance on past capacity signals is higher under immediate pricing for the second sub-period than under average pricing.

This subsection has derived, in closed form, how BRPs and the TSO adjust their actions differently across sub-periods 1 and 2, given their respective information sets. Section 4.2.1 extends the comparative analysis to all five pricing mechanisms.

4.1.2 BRP Behaviour to Decrease in Marginal Cost of Adjustment

We expect the BRPs to rely more heavily on the last value of activated capacity (β_1 and β_2) if their cost of adjustment θ decreases. Lower θ makes it cheaper for the BRPs to adjust, so they respond more strongly to capacity signals. By contrast, a higher θ forces BRPs to be more cautious before adjusting their intentional imbalance.

This economic intuition is shown by looking at the partial derivatives $\partial\beta_1/\partial\theta$ and $\partial\beta_2/\partial\theta$.

For the immediate pricing:

$$\frac{\partial\beta_1}{\partial\theta} = \frac{\partial\beta_2}{\partial\theta} = -\frac{\rho\gamma}{(\theta+\gamma)^2} < 0 \quad \text{given } \gamma > 0,\ \rho > 0 \tag{4.11}$$

While for the average pricing:

$$\frac{\partial \beta_1}{\partial \theta} = -\frac{2\gamma\rho(1+\rho)}{(2\theta+2\gamma)^2} < 0 \quad \text{given } \gamma > 0,\ \rho > 0 \tag{4.12}$$

$$\frac{\partial \beta_2}{\partial \theta} = -\frac{2\gamma(1+\rho)}{(2\theta+\gamma)^2} < 0 \quad \text{given } \gamma > 0,\ \rho > 0 \tag{4.13}$$

Since the partial derivative of the parameter related to the last observed capacity with respect to θ is strictly negative, a decrease in the value of θ causes β_1, β_2 to increase in the two pricing mechanisms.

Computing the partial derivative for β_3 and β_4 we note that they also increase with a decrease in θ.

This result is in line with the current market situation, where the expansion of BESS as a way to store energy drastically reduced the cost of adjustment for the BRPs (θ), resulting in an increase in the intentional deviation from the BRPs. Under the right incentives, this can force BRPs to intentionally deviate more, increase the share of passive balancing, and reduce the overall system deviation. This view is supported by the literature and explained in detail in Section 2.3.

4.1.3 TSO Response to a Decrease in BRP Marginal Cost

Similarly, we can look at the effect of a decrease in the BRPs' marginal cost of balancing on the TSO behaviour.

In this case we compute the partial derivative of α_1, α_2 with respect to θ for the immediate pricing as:

$$\frac{\partial \alpha_1}{\partial \theta} = \frac{\partial \alpha_2}{\partial \theta} = \frac{\rho\gamma}{(\theta+\gamma)^2} > 0 \quad \text{given } \gamma > 0,\ \rho > 0 \tag{4.14}$$

Similarly for the average pricing:

$$\frac{\partial \alpha_1}{\partial \theta} = \frac{2(2\theta+2\gamma) - 2(2\theta+\gamma-\gamma\rho)}{(2\theta+2\gamma)^2} = \frac{2\gamma(1+\rho)}{(2\theta+2\gamma)^2} > 0 \quad \text{given } \gamma > 0,\ \rho > 0 \tag{4.15}$$

$$\frac{\partial \alpha_2}{\partial \theta} = \frac{2\rho(2\theta+\gamma) - 2(2\theta\rho-\gamma)}{(2\theta+\gamma)^2} = \frac{2\gamma(1+\rho)}{(2\theta+\gamma)^2} > 0 \quad \text{given } \gamma > 0,\ \rho > 0 \tag{4.16}$$

From these derivations we conclude that the TSO positively responds to an increase in θ, which means that they negatively respond to a decrease in the marginal cost. This result is supported by the logic that TSOs need to counterbalance the deviation made by the BRPs. For this reason, with lower cost of adjustment BRPs will have more flexibility to intentionally deviate and correct the system imbalances through passive balancing, requiring less action from the TSO, hence the positive relationship $\partial\alpha/\partial\theta > 0$.

4.2 Simulation Results

Rule	Immediate	Average	End	Dual	Cond_dual
α_1	0.3472 (0.31)	0.3723 (0.35)	0.4372	0.3426	0.3371
α_2	0.3335 (0.31)	0.0604 (-0.01)	0.3365	0.0601	0.0600
α_3	0.1977 (0.17)	0.4148 (0.39)	0.3292	0.3495	0.3484
α_4	0.1873 (0.17)	0.1946 (0.22)	0.1468	0.1506	0.1423
β_1	0.5941 (0.54)	0.5131 (0.50)	0.4709	0.5495	0.5568
β_2	0.5212 (0.54)	0.8874 (0.86)	0.5302	0.8874	0.8874
β_3	0.3413 (0.29)	0.3913 (0.34)	0.2177	0.4675	0.4694
β_4	0.3551 (0.29)	0.1915 (0.198)	0.2615	0.2716	0.2857
RMS A^2	18.4767	18.2808	18.1434	18.5294	18.5528
BRP Costs	3155.3609	2734.8005	3647.9083	4190.3523	4180.4621
$\mathbb{E}[\gamma c^2/2]$	1380.0803	1363.9131	1518.9800	1314.1809	1310.9052
$\mathbb{E}[\theta x^2/2]$	462.3510	587.6735	369.6461	624.7249	629.9941
System Cost	1842.4313	1951.5866	1888.6261	1938.9057	1940.8993
$\mathbb{E}[px]$	927.6964	1188.3604	741.0366	1393.5828	1420.1411
$\mathbb{E}[p\mu]$	-3620.7063	-3335.4873	-4019.2988	-4959.2103	-4970.6091
σ_c (ISP)	28.9318	25.9213	30.7764	25.1894	25.1143
ρ_c (lag 1)	0.4604	0.5098	0.5756	0.4395	0.4324
σ_p (ISP)	130.9020	117.2808	157.5213	188.5408	189.7684
$\sigma_{x+\mu}$ (ISP)	45.6882	43.4598	46.3250	43.3598	43.3588
Regstate2 (%)	37.6%	46.5%	37.1%	47.1%	47.4%

Table 4.1: Simulation Results by Pricing Rule. Parameters used: $\sigma_\epsilon = 17.8482$, $\rho_\mu = 0.85/7\text{min}$, $\gamma = 9.0490$, $\theta = 5.1768$ — achieved via the simulation technique described in Section 3.3. In parentheses: analytical results where applicable.

Note: RMS A^2 refers to the Root-mean-square of A^2; a summary measure of average squared ACE over all simulated ISPs. $\mathbb{E}[\gamma c^2/2]$ is the expected TSO cost for capacity activation and $\mathbb{E}[\theta x^2/2]$ the expected BRP cost for intentional deviation. The sum of them is the system cost. Regulation State 2 are the ISPs where the capacity activated in one of the two time period is positive and negative the other one.

4.2.1 BRPs Response to Available Information

Under different pricing mechanisms the information acquired by the BRP at the beginning of the second time period plays different roles. For example, in the end pricing p_T is determined solely by c_2, thus BRPs have higher incentive to optimise their

deviation in $t = 2$. This intuition is reflected by high values for β_2^{end} and β_4^{end} (from Table 4.1: $\beta_2^{\text{end}} = 0.53$, $\beta_4^{\text{end}} = 0.26$), compared to other pricing mechanisms.

This logic explains why $\beta_2^{\text{end}} > \beta_1^{\text{end}}$ and $\beta_4^{\text{end}} > \beta_3^{\text{end}}$: BRPs defer most of their correction to the second subperiod. Yet the same feature, setting p_T solely on c_2, also means that any shock hitting c_2 is fully transmitted to p_T, amplifying price volatility and dampening BRP's willingness to intentionally deviate. This effect appears in the results as a higher σ_p^{end} compared to other single pricing rules (i.e., immediate and average pricing), and lower values of β parameters compared to the other four pricing rules.

Furthermore, because in the second time period both end and immediate pricing tie the price exclusively to c_2, BRPs face similar forecasting uncertainty in sub-period 2 under these rules (from Table 4.1 $\beta_2^{\text{end}} \approx \beta_2^{\text{imm}}$). Consequently, the TSO's reaction, α_2, is higher under these pricing rules, reflecting heavier active balancing. The share of active balancing is measured through σ_c, which peaks under end pricing and is second highest under immediate pricing. The higher volatility under end compared to immediate pricing arises because BRPs have no incentive to correct in period 1, since it is not going to determine the imbalance price, while under immediate pricing the BRPs have the same incentives in the first and second subperiod.

Figure 7.5 illustrates this mechanism: under both end- and immediate-pricing rules, BRPs respond less to extreme shocks.

This similarity between the end and the immediate pricing in t=2 make the end pricing the rule with the lowest system cost (Table 4.1 and Figure 7.4). This is the case because the final price is determined solely by capacity activated in the second sup-period, without the need for BRPs to over-react to avoid higher penalties (as happens under the dual pricing).

In contrast to the end and immediate pricing schemes, in the remaining three mechanisms the information gained at the end of $t = 1$ is extremely useful to the optimization of x_2. As discussed in Section 4.1.1, BRPs therefore adopt a more cautious approach in the first subperiod to overcorrect in the second.

4.2.2 Penalty as Incentive to Correct Deviation

As explained in Section 2.4.3, some pricing mechanisms incentivise BRPs to correct unintentional deviations internally. This is done with the use of penalties.

For example, under dual pricing, BRPs pay the highest of the two sub-period prices whenever the total capacity activated is positive, providing a strong incentive to help the system correct unintentional shocks. Especially under extreme shocks, dual pricing drives the imbalance price up more than in other rules, such as the average pricing ($\sigma_p^{\text{dual}}, \sigma_p^{\text{cond}} > \sigma_p^{\text{others}}$).

This forces the BRPs to take the burden of the unintentional shock and correct the system in the second sub-period. As a result, the parameter β_2^{dual} reaches its highest values across all mechanisms. The equality of $\beta_2^{\text{dual}} = \beta_2^{\text{cond}} = \beta_2^{\text{avg}} = 0.89$ reflects that all three pricing mechanisms share the same end-period corrective logic (Section 4.2.1), although they implement different cost structures.

Consequently, under dual and conditional dual pricing, the BRPs incur high expected adjustment costs, $\mathbb{E}[\frac{1}{2}\theta x^2]$, leading to the high net imbalance expenses under these pricing mechanisms. These corrections, while costly, help the system to keep the lowest imbalance volatility ($\sigma_{x+\mu}$).

The key downside of stronger BRP reactions, however, is the increase in regulation state 2 events occurring. The occurrence of this regulation state forces BSPs to activate both positive and negative capacity within the same ISP. In such cases, a strong BRP correction can flip the system imbalance within the same ISP, triggering BSP's undesired reserve swing.

As a result, although dual pricing ensures higher expected TSO revenue (as shown by high $\mathbb{E}[px]^{\text{dual}}, \mathbb{E}[px]^{\text{cond}}$), it also incurs the highest expected cost of balancing unintentional deviation $\mathbb{E}[p\mu]$, reflecting elevated expenses in both passive and active corrections.

4.2.3 Residual ACE Driven by Unpredictable Shocks

The main finding of this thesis is that residual ACE, after active and passive balancing, is driven by the unpredictable shock, instead of the choice of pricing rule. Figure 7.2 visually shows this result. Regardless of the pricing rule, the residual ACE closely mirrors the unpredictable shock ϵ, almost zeroing out the predictable component. Consequently, incremental adjustments to pricing mechanisms offer limited scope for further stability; substantive reductions in residual ACE can be achieved only through policies that lower forecast error and, by extension, the variance of the shock itself.

Table 4.1 numerically confirms this result, where the value of RMS A^2 among different pricing mechanisms is similar and converges to the value of σ_ϵ, the standard deviation of the shock.

Analytically, the TSO policy functions (Equations 3.7 and 3.8) incorporate information on the most recent two periods to forecast and offset the expected imbalance. This ensures that, conditional on past information, the expected ACE is zero (following the explanation in Section 3.1.1):

$$\mathbb{E}[A_t \mid t{-}1] = 0 \tag{4.17}$$

To maintain analytical tractability, we neglected deeper lags ($k > 2$). As explained in Section 3, this simplified the derivation, leaving the variance unchanged. In principle, with full historical information on the system imbalance and activated capacity, the TSO could perfectly offset the predictable imbalance, leaving only the unpredictable component:

$$A_t = \epsilon_t \tag{4.18}$$

The key implication of the analysis is that this result is independent of the pricing rule implemented, with only minor differences in the value of A^2 that do not alter the overall conclusion. Different pricing rules influence the behavioural parameters α and β, shifting the balancing action to the participants with lower marginal costs, modifying the relative contribution to active and passive balancing (Section 4.2.1 and 4.2.2), while

keeping the same aggregate feedback loop that effectively eliminates the predictable component.

This implies that the role of the pricing mechanism is not to enhance the system's ability to correct imbalances, which is achieved through the feedback loop, but rather to determine how the cost of the residual shock ϵ is allocated across market participants. Importantly, this conclusion is derived from explicitly specified and policy-relevant behavioural rules (Equations 3.14–3.15 and 3.7–3.8) for both the TSO and BRPs.

In this sense, the pricing rule functions as a cost-distribution mechanism: it defines whether imbalance costs are primarily absorbed by BRPs through passive balancing or by the TSO through the instruction of BSPs.

Chapter 5

Discussion

Q1: impact on ACE As shown in Section 4.2.3, in our model changing pricing mechanisms is not effective to decrease ACE. All the mechanisms give us roughly the same results: the market participants arbitrage away deterministic ACE components, leaving the residual of ACE to the unexpected shock ϵ_t.

Under this result, once we define a stable feedback equilibrium, no matter if it is under end, average, or dual pricing, changing the financial settlement does not change the result under the goal of minimising ACE. This result corroborates the finding discussed in Pierro et al. (2022), which calls for improvements in the forecasting system to reduce the system imbalances. Consequently, policies should prioritise lowering σ_ϵ, for example through better VRE forecasting, rather than focusing on the pricing rule implemented.

For this, however, a stable feedback equilibrium is required. This means that BRPs and TSO can form expectations on intentional deviation and reserve activation, almost zeroing out the predictable component of ACE.

Q2: BRPs, TSO, and system costs and cost shifting According to these results, the TSO's discussion around which pricing mechanism to adopt should focus on the market participants bearing the cost for the residual ACE. As evaluated in Sections 4.2.1 and 4.2.2, different pricing mechanisms substantially change the BRPs and TSO costs and the share of active and passive balancing.

Choosing a dual pricing mechanism or a conditional dual pricing one forces the BRPs to react more heavily by increasing the penalty for each deviation. Under these mechanisms the BRPs take the burden for all the unintentional deviation caused, increasing their cost. On the other hand, choosing the end rule forces the TSO to increase the level of BSPs' reserve activation to counterbalance the unpredictable shock. Overall, as explained in Section 4.2.1 the end pricing results in lower system cost.

These results support the results found in Helander et al. (2010) and Wu et al. (2020) on the higher system cost of the dual pricing mechanisms and the lack of incentive of the single pricing mechanisms described in Koch and Maskosa (2019) and Koch (2021).

Q3: Role of BESS Moreover, the thesis evaluated the recent impact of a decrease in the marginal cost of adjustment for the BRPs. With the increasing importance of BESS in the market, BRPs can change their intentional position easily and incur lower costs of adjustment (Jaffal et al., 2024; Padmanabhan et al., 2019). In our model this decrease is captured by a reduction in θ. As shown in Sections 4.1.2 and 4.1.3 and Figure 7.8, a decrease in θ gives higher incentives for the BRPs to deviate more to balance the unintentional deviation.

This higher response is well targeted: since the covariance between the intentional and unintentional deviation becomes more negative, the BRPs react more and better (Section 7.3.4). This indicates that widespread deployment of BESS systems can shift the burden of correcting system imbalance by allowing BRPs to absorb VRE-driven shocks quickly and at lower cost. Despite this, the BESS cannot help to decrease the overall system imbalance, which is driven by the ability to forecast VRE production. This result is in contrast with the finding in Smets et al. (2023) where BESS helped the system to reduce the system imbalance.

Policy Implication The findings point to three actionable policy priorities for the Dutch balancing market. First, because residual ACE is driven by ϵ, incremental adjustments to the pricing rule cannot deliver further stability gains. Regulatory effort should therefore pivot toward the improvement of forecasting tools that lower the variance of VRE forecast error.

Second, given that all five pricing rules leave ACE unchanged yet redistribute costs very differently, the choice of settlement rule is a distributional decision rather than an efficiency lever. End pricing place a larger share of balancing cost on the TSO, whereas dual and conditional-dual pricing shift the burden to BRPs through steeper imbalance penalties. Policymakers should therefore select the rule that best aligns with their equity objectives and specific goals.

Third, the analytical results shows that a lower adjustment cost θ increases BRP corrections without inducing over-correction, enabling the TSO to rely on smaller reserve volumes. Targeted incentives for BESS integration (e.g., reduced connection fees or priority dispatch) would thus reduce total system costs even if ACE variance itself is unchanged.

Limitation However, our analytical framework relies on simplified assumptions to enable a closed-form solution of our model. These assumptions might limit the direct applicability of our model to real-world scenarios.

Firstly, we assumed homogeneous atomic BRPs who do not have any power to influence the market price. However, BRPs differ in size, energy produced, and geographical location. This might influence their strategic decision on the intentional deviation to shift the price to a more convenient level. The BRPs' geographical location can also be added in our model, designing the unintentional deviation as a vector autoregressive model instead of a simpler AR(1). A vector autoregressive model would be effective to relax the assumption of homogeneous BRPs, allowing for different impacts of the shock

on different BRPs. For example, it would allow us to consider the difference between a solar plant in the southern region and a wind plant in the north.

Furthermore, we evaluated a simplified version of the market structure, with two time periods in the ISP and no transboundary trade. Expanding this model to a 15-minute ISP and allowing for transboundary trade will change the model structurally. Transboundary trade requires a cross-country approach, where different areas need to be analysed with the capacity flow between them. In this case, the BRPs and TSO will not decide only based on the values of previous activated capacity, but they will also include the previous value of trade inflow or outflow.

Chapter 6

Conclusion

This thesis asked whether alternative imbalance pricing rules can (i) lower equilibrium Area Control Error (ACE); (ii) minimise balancing costs for the TSO, BRPs, and the system as a whole; and (iii) be complemented by battery-storage deployment to enhance system performance. A closed-form feedback model, supported by simulation with Dutch calibration, yields robust insights.

Once a stable feedback equilibrium is in place, BRPs and the TSO arbitrage away every predictable component of ACE, so residual imbalance equals the VRE-driven shock under all five pricing rules. Further stability therefore hinges on reducing forecast error, not on the choice of the pricing rule. Thus, regulators should treat settlement choice as a distributional lever, selecting the rule that matches equity objectives rather than efficiency goals.

However, this work leaves room for future improvement in the evaluation of alternative pricing mechanisms and the expansion of the model through the relaxation of various assumption made.

Chapter 7

Appendix

7.1 Simulation Code

Remark: The code used for the simulation and the calibration can be found on GitHub following this link: GitHub Repository

7.1.1 Code

Parameter and Initialization After importing the relevant packages, we set the parameters values for $\gamma, \theta, \sigma_\epsilon, \rho$ and 1000 time period. We also set the seed and simulate the value of the unpredictable shock, ϵ. We used a seed value to allow for applicability.

Definition of Pricing Rules class We create a class called PricingRules, where we plug in all the pricing mechanisms we want to compare in our analysis. In this section we just define the class, the specifics of each pricing mechanism are defined later in the simulate function. Definition of other relevant classes We encapsulated all the relevant parameters for our model into classes:

- `ScenarioInputs` stores parameters (α, β, ϵ, pricing rule),
- `ScenarioOutputs` stores time-series variables (e.g. capacity, imbalance, price). Note that in the simulation we used x as intentional deviation and μ as the unintentional one,
- ScenarioStatistics aggregates relevant simulation outcomes (e.g. BRP and TSO cost and expenses, ...),
- `ScenarioCalibration` contained the relevant value for calibration and comparison with realworld data ($\sigma_c, \sigma_p, \sigma_{x+\mu}, \rho_c$)

After that Scenario binds everything into a single run context.

Definition of the function We then define the simulate function to generate the state evolution over time (Equations 3.2, 3.3, 3.4, 3.7, and 3.8) and the `sim_plus_prices` to include different pricing mechanisms (Listing 7.1). We also defined relevant functions for Asquared and BRP cost, needed for the BRP and TSO optimisation. The last function we defined is `find_equilibrium` which solves the model by alternating optimization of α and β under different pricing rules.

Iteration over pricing Rule I then solve the model and store the relevant results and statistics in the list `results`.

Showing results Last part of the code store the results in a data frame and show different tables and graphs

7.1.2 Different Pricing Mechanisms

```
def sim_plus_prices(s_input: ScenarioInputs) -> ScenarioOutputs:
    s_output = simulate(s_input)
    rule = s_input.rule
    mu, c, x, a, p = s_output.mu, s_output.c, s_output.x, s_output.a,
        s_output.p
    if rule == PricingRules.immediate:
        p[:,0] = gamma * c[:,0]
        p[:,1] = gamma * c[:,1]
    elif rule == PricingRules.average:
        avg = 0.5 * gamma * (c[:,0] + c[:,1])
        p[:] = avg[:,None]
    elif rule == PricingRules.end:
        p[:] = gamma * c[:,1][:,None]
    elif rule == PricingRules.dual:
        net = (x + mu).sum(axis=1)
        mask_down = net > 0
        mask_up   = net <= 0
        p_down = gamma * np.min(c, axis=1)
        p_up   = gamma * np.max(c, axis=1)
        p[mask_down] = p_down[mask_down, None]
        p[mask_up]   = p_up[mask_up, None]
    elif rule == PricingRules.cond_dual:
        net = (x + mu).sum(axis=1)
        mask_pp = (c[:,0] > 0) & (c[:,1] > 0)
        mask_nn = (c[:,0] < 0) & (c[:,1] < 0)
        mask_mp = ~(mask_pp | mask_nn) & (net >= 0)
        mask_mn = ~(mask_pp | mask_nn) & (net < 0)
        price_max = gamma * np.maximum(c[:,0], c[:,1])
        price_min = gamma * np.minimum(c[:,0], c[:,1])
        p[mask_pp] = price_max[mask_pp, None]
        p[mask_nn] = price_min[mask_nn, None]
        p[mask_mp] = price_min[mask_mp, None]
        p[mask_mn] = price_max[mask_mn, None]
```

Listing 7.1: Example Python Function

The underlining rule of different pricing is explained in the Section 1. In the simulation we followed the same structure. For each ISP the price is a vector of length=2, which needs to be filled with the settlement price during that period. In all the pricing mechanisms except for the immediate pricing, the two values in the vector are the same. In the immediate pricing, the first term refers to the sub-period pricing in the first time period, while the second term to the second sub-period price. For the dual and conditional dual pricing, we used mask, to map each specific scenario and set the price as the maximum or the minimum activated capacity. Note that when the final price has only one column, Python automatically reshape it to follow the defined shape (Tmax,2).

7.2 Calibration of the Parameters

From TenneT we have ISP data on the imbalance price and volume per ISP, and the capacity activated per minute. Since our model assume 2 sub-periods per each ISP, we calibrate the data aggregating the values per ISP. From the data we first did a sanity check, making sure that the unit of measurement are consistent and that the values, especially for downward adjustments, have the same sign.

We then computed the standard deviation and the autocorrelation of the capacity, and the standard deviation of the imbalance using the function .std and .autocorr for the already aggregated measure[1].

For the price it is trickier since the Dutch market uses single or dual pricing depending on the state regulation. When regulation state 2 occurs, we flatten the values and compute the standard deviation on the results. We iterated for a number of 20 iterations with the learning rate of 0.1. To calibrate the parameters, we use the following iteration scheme:

$$\sigma_{\epsilon}^{n} \leftarrow \left(\frac{\sigma_{c}^{d}}{\sigma_{c}^{m}}\right)^{\lambda} \sigma_{\epsilon}^{c} \tag{7.1}$$

$$x_{\mu}^{n} \leftarrow x_{\mu}^{c} + \lambda\left(x_{\mu}^{d} - x_{\mu}^{m}\right) \tag{7.2}$$

$$\gamma^{n} \leftarrow \left(\frac{\sigma_{p}^{d}}{\sigma_{p}^{m}}\right)^{\lambda} \gamma^{c} \tag{7.3}$$

$$\theta^{n} \leftarrow \left(\frac{\sigma_{x+\mu}^{m}}{\sigma_{x+\mu}^{d}}\right)^{\lambda} \frac{\gamma^{n}}{\gamma^{c}} \theta^{c} \tag{7.4}$$

In the iteration, the superscript n stands for next iteration, superscript c for current iteration, superscript d for observed data, and superscript m for model results.

Furthermore, x_{μ} is defined as:

$$x_{\mu} = \ln(\rho_{\mu}) - \ln(1 - \rho_{\mu}) \tag{7.5}$$

[1]The function .std computes the standard deviation and .autocorr computes the correlation.

With:

$$\rho_\mu = \frac{e^{x_\mu}}{1 + e^{x_\mu}} \tag{7.6}$$

We clipped the value of ρ to 0.85 to avoid overflowing issues when running the simulation. For this reason, we were not able to get close to the real value of ρ_c.

Furthermore, decreasing θ should bring the value of σ_x up, as explained in Section 4, however the value of $\sigma_{x+\mu}$ does not decrease accordingly (figure 7.1 for reference). For this reason, the value of $\sigma_{x+\mu}$ cannot be set closer. The reason for this non decreasing in $\sigma_{x+\mu}$ is given by the derivation of the variance:

$$Var(x + \mu) = Var(x) + Var(\mu) + 2Cov(x; \mu) \tag{7.7}$$

As the variance of x increase and the variance of the sum does not, the covariance between the two measure decreases. This intuition is explained in Section 7.3.4.

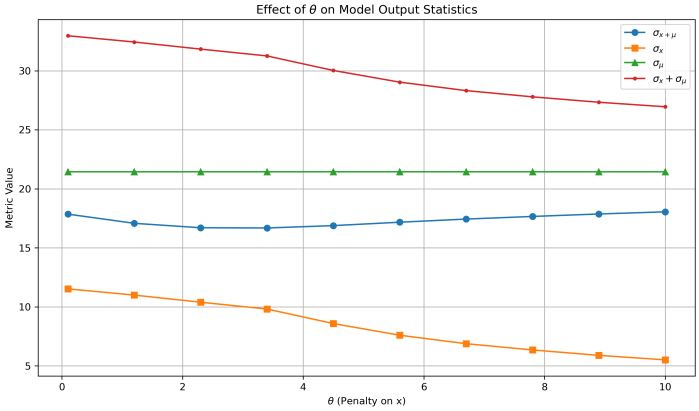

Figure 7.1: Change in the values of σ with change in θ under the conditional dual pricing

7.3 Additional Figures and Results

7.3.1 Area Control Error

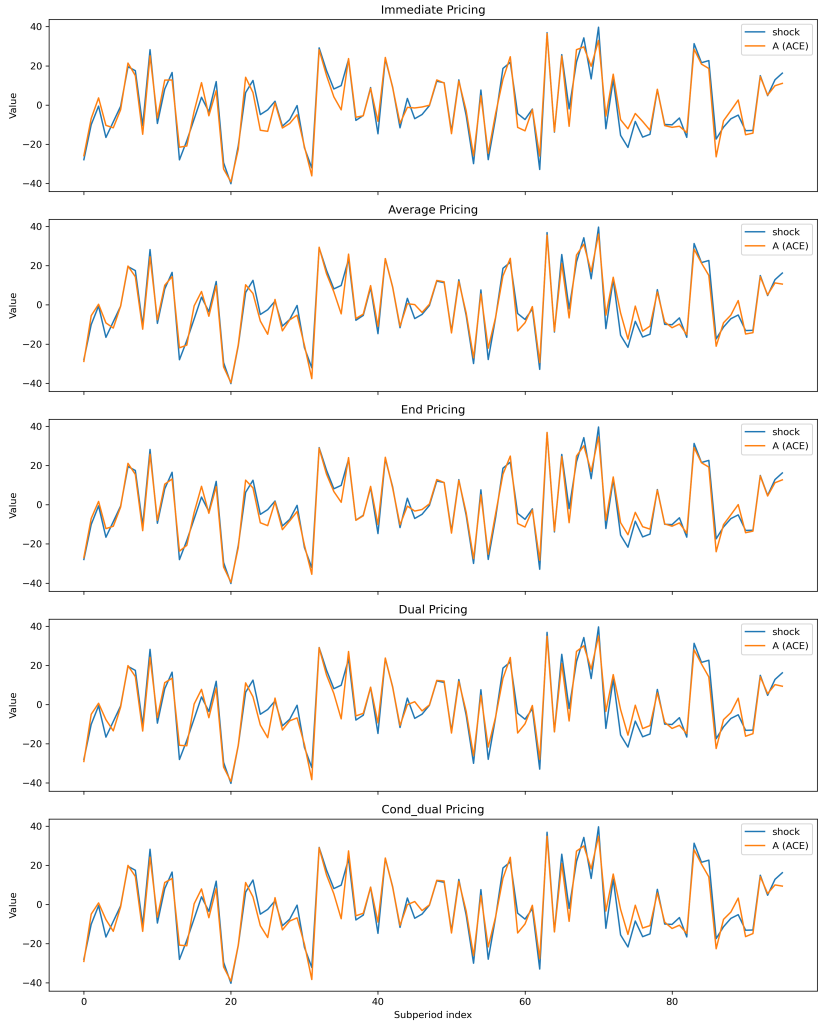

Figure 7.2: Plot of ACE and ϵ under the five different pricing mechanisms

As explained in section 4 the TSO under different pricing mechanisms can almost perfectly zero out the predicable component of ACE. This graph shows that despite slight difference, the residual ACE mirror the unexpected shock.

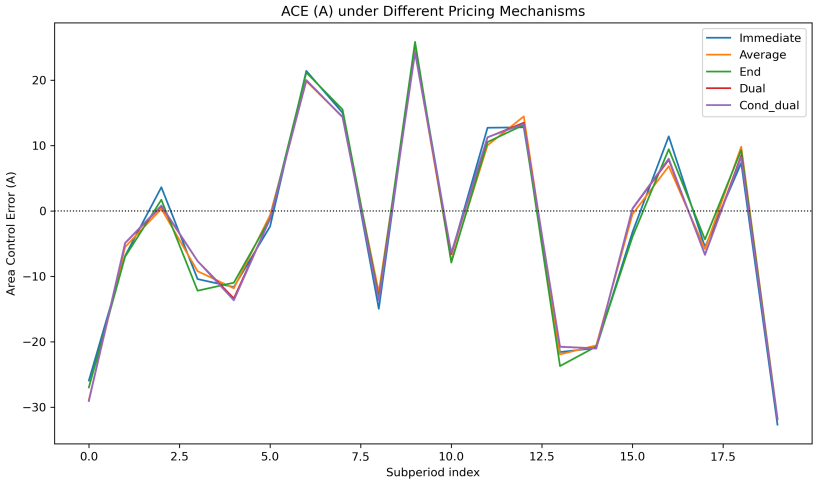

Figure 7.3: Variation of ACE under the five pricing mechanisms evaluated

Although pricing mechanisms influence BRP expectations and capacity activation patterns, their impact on the Area Control Error (ACE) remains limited. As also discussed in Section 4, the figure confirms that ACE exhibits minimal variation across pricing rules, suggesting that TSO response is effective in maintaining system stability regardless of pricing design.

7.3.2 System Cost

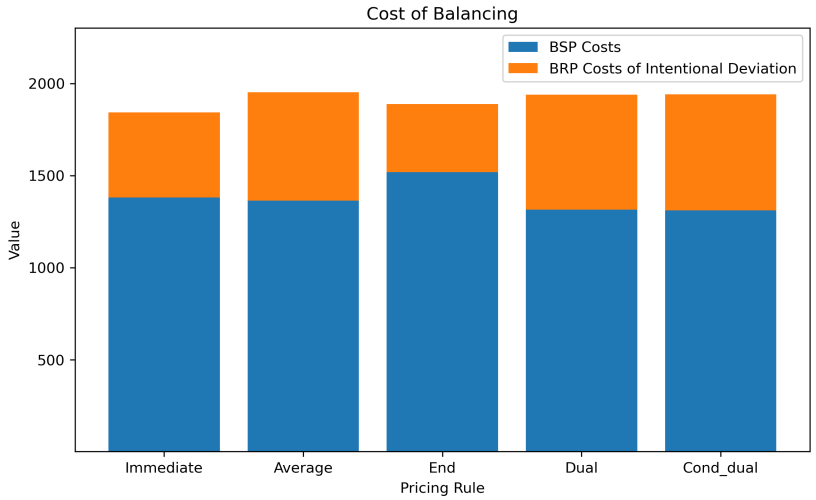

Figure 7.4: Breakdown of total balancing cost under different pricing mechanisms. The blue bars represent BSP (TSO) costs from activated balancing capacity, while the orange bars reflect BRP costs from intentional deviation penalties.

This figure provides a comparative breakdown of total system costs across pricing mechanisms, highlighting how each rule allocates the economic burden between BRPs and the TSO. The End pricing rule results in a higher total cost, driven by a spike in TSO

balancing requirements. While the Dual and Conditional Dual mechanisms produce similar aggregate costs, they impose a greater share on BRPs, reflecting stronger deterrent incentives (Section 4.2.2).

7.3.3 Intentional deviation and capacity

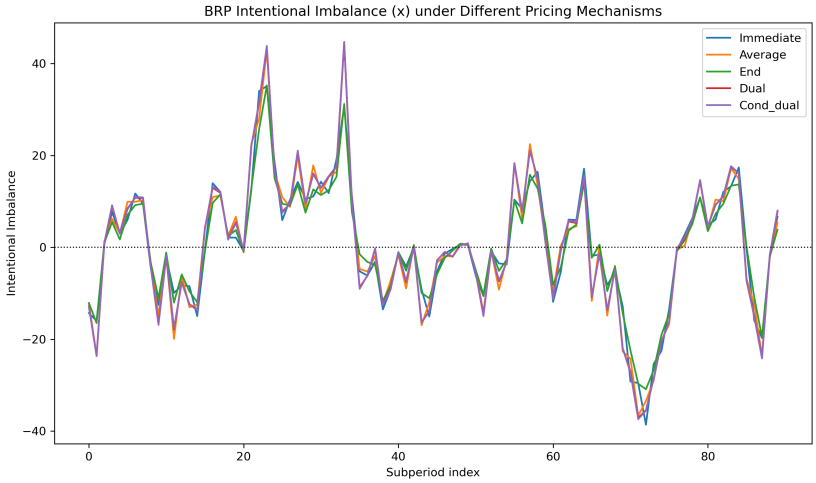

Figure 7.5: Intentional deviation (x_t) of BRPs across different pricing mechanisms.

The figure illustrates how BRPs adjust their intentional imbalances under varying pricing rules. As discussed in Section 4, under the end-of-period and immediate pricing regimes, BRPs tend to underreact to market conditions, particularly in the presence of extreme shocks, due to increased forecast uncertainty and delayed pricing signals.

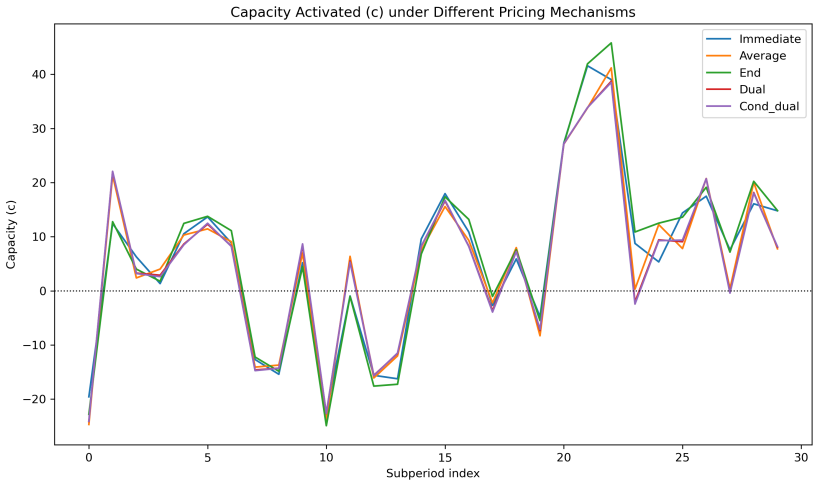

Figure 7.6: Capacity activation (c_t) across 30 subperiods under the five different pricing mechanisms

This figure illustrates how the Transmission System Operator (TSO) adjusts real-time balancing capacity in response to market conditions under each pricing rule. While

the overall structure and volatility of capacity activation are broadly preserved across mechanisms, the End and Conditional Dual pricing rules exhibit slightly stronger adjustments in response to extreme imbalances. This suggests that mechanisms that delay or condition pricing signals can induce larger corrective actions from the TSO, likely due to the strategic underreaction of BRPs observed under those rules (see Figure 7.5).

7.3.4 Effects of Variation of θ and γ

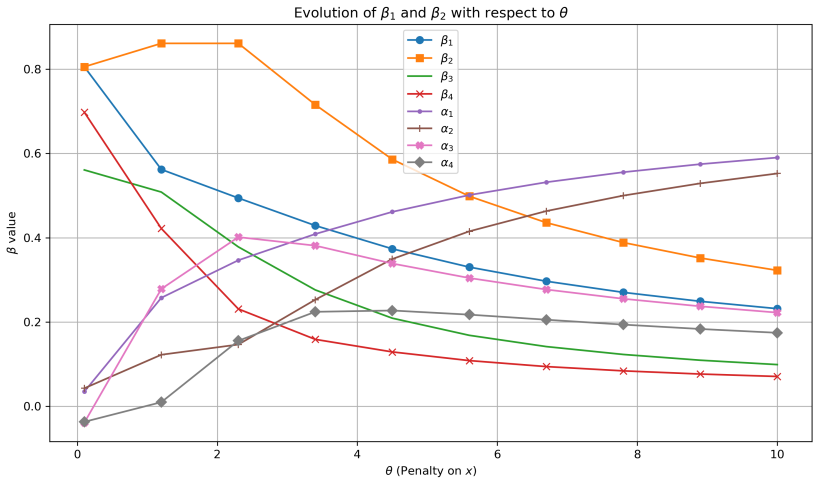

Figure 7.7: Effect of increasing penalty on intentional deviation (θ) on model feedback parameters β_i and α_i. Parameters used: $\rho = 0.85, \sigma_\epsilon = 12, \gamma = 4$

This figure illustrates how the feedback parameters that govern the interaction between BRP expectations and TSO response evolve with respect to θ, the marginal cost of intentional imbalance. As θ increases, BRPs become more conservative in their deviations, which is reflected in the decreasing values of β_1 and β_2 — these capture the BRP's behavioural sensitivity to previous capacity levels (Section 4.1.2 and Figure 7.1). Conversely, the corresponding α_1 and α_2, which shape TSO capacity policy, increase. This reflects the TSO compensating for BRP passivity by relying more heavily on past imbalances (Section 4.1.3). The convergence trend visible in higher θ values confirms the expected trade-off: stronger penalisation reduces strategic responsiveness, requiring more reactive system-level control.

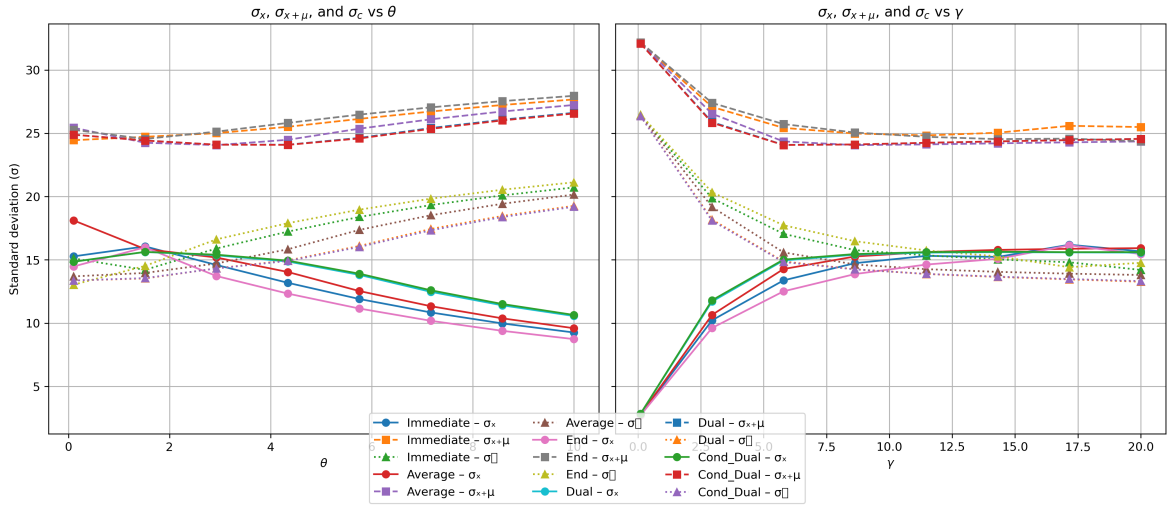

Figure 7.8: Effect of marginal cost parameters θ (left) and γ (right) on the standard deviation of key model outcomes: BRP intentional imbalance σ_x, total imbalance $\sigma_{x+\mu}$, and activated capacity σ_c, under five different pricing mechanisms. Parameters used $\rho = 0.85, \sigma_\epsilon = 12$ On the left $\gamma = 5$, on the right $\theta = 4$.

This figure shows how the standard deviations of the main endogenous variables respond to changes in BRP marginal cost of intentional deviation (θ) and TSO balancing cost (γ). On the left, we observe that decreaseing θ (i.e., incentivising BRP's deviation) causes a clear increase in σ_x, which aligns with the analytical results in Section 4.1.2. This increase in BRP's intentional deviation is followed by a decrease in the capacity activated ,σ_c for the reason found in 4.1.3. The intersting results is that, despite the increase in σ_x, the variance of the total deviation does not drastically change. This suggest a sharp decrease in the $Cov(x;\mu)$ to keep:

$$Var(x+\mu) = Var(x) + Var(\mu) + 2Cov(x;\mu) \tag{7.8}$$

constant. A decrease in the covariance, which is already negative, suggests that BRPs react better to counterbalance the unintentional shock. On the right, increasing γ reduces σ_c sharply at first, but the effect vanish beyond $\gamma > 10$.

Bibliography

Acaroğlu, H. and García Márquez, F. P. (2021). Comprehensive review on electricity market price and load forecasting based on wind energy. *Energies*, 14:7473.

Angenendt, G., Merten, M., Zurmühlen, S., and Sauer, D. U. (2020). Evaluation of the effects of frequency restoration reserves market participation with photovoltaic battery energy storage systems and power-to-heat coupling. *Applied Energy*, 260:114186–114186.

Backer, M., Keles, D., and Kraft, E. (2023). The economic impacts of integrating european balancing markets: The case of the newly installed afrr energy market-coupling platform picasso. *Energy Economics*, 128:107124.

Commission, E. (2017a). Eur-lex - 02017r2195-20210315 - en - eur-lex.

Commission, E. (2017b). Regulation - 2017/1485 - en - eur-lex.

Ehrhart, K.-M. and Ocker, F. (2021). Design and regulation of balancing power auctions: an integrated market model approach. 60:55–73.

ENTSO-E. Manually activated reserves initiative.

ENTSO-E. Picasso.

ENTSO-E (2016). Imbalance netting.

ENTSO-E (2017). Terre.

Goodarzi, S., Perera, H. N., and Bunn, D. (2019). The impact of renewable energy forecast errors on imbalance volumes and electricity spot prices. *Energy Policy*, 134:110827.

Haring, T. W., Kirschen, D. S., and Andersson, G. (2015). Incentive compatible imbalance settlement. *IEEE Transactions on Power Systems*, 30:3338–3346.

Helander, A., Holttinen, H., and Paatero, J. (2010). Impact of wind power on the power system imbalances in finland. *IET Renewable Power Generation*, 4:75.

Herrera de Silva, P. and Horta, P. (2018). The effect of variable renewable energy sources on electricity price volatility: The case of the iberian market. *SSRN Electronic Journal*.

Hirth, L. and Ziegenhagen, I. (2013). Balancing power and variable renewables: A glimpse at german data. *SSRN Electronic Journal*.

Jaffal, H., Guanetti, L., Rancilio, G., Spiller, M., Bovera, F., and Merlo, M. (2024). Battery energy storage system performance in providing various electricity market services. *Batteries*, 10:69–69.

Just, S. and Weber, C. (2008). Pricing of reserves: Valuing system reserve capacity against spot prices in electricity markets. *Energy Economics*, 30:3198–3221.

Kazmi, H. and Tao, Z. (2022). How good are tso load and renewable generation forecasts: Learning curves, challenges, and the road ahead. *Applied Energy*, 323:119565.

Koch, C. (2021). Intraday imbalance optimization: incentives and impact of strategic intraday bidding behavior. *Energy Systems*, 13:409–435.

Koch, C. and Maskosa, P. (2019). Passive balancing through intraday trading. *SSRN Electronic Journal*.

Miettinen, J. and Holttinen, H. (2019). Impacts of wind power forecast errors on the real-time balancing need: a nordic case study. *IET Renewable Power Generation*, 13:227–233.

Miettinen, J., Holttinen, H., and Giebel, G. (2014). Nordic wind power forecast errors : benefits of aggregation and impact.

Obersteiner, C., Siewierski, T., and Andersen, A. N. (2010). Drivers of imbalance cost of wind power: A comparative analysis. *International Conference on the European Energy Market*.

Padmanabhan, N., Ahmed, M., and Bhattacharya, K. (2019). Battery energy storage systems in energy and reserve markets. *IEEE Transactions on Power Systems*, pages 1–1.

Pierro, M., Liolli, F. R., Gentili, D., Petitta, M., Perez, R., Moser, D., and Cornaro, C. (2022). Impact of pv/wind forecast accuracy and national transmission grid reinforcement on the italian electric system. *Energies*, 15:9086.

Poplavskaya, K., Lago, J., and de Vries, L. (2020). Effect of market design on strategic bidding behavior: Model-based analysis of european electricity balancing markets. *Applied Energy*, 270:115130.

Roben, F. and de Haan, S. (2019). Market response for real-time energy balancing – evidence from three countries. *2022 18th International Conference on the European Energy Market (EEM)*, pages 1–5.

Roumkos, C., Biskas, P. N., and Marneris, I. G. (2022). Integration of european electricity balancing markets. *Energies*, 15:2240–2240.

Shinde, P., Hesamzadeh, M. R., Date, P., and Bunn, D. W. (2021). Optimal dispatch in a balancing market with intermittent renewable generation. *IEEE Transactions on Power Systems*, 36:865–878.

Smets, R., Bruninx, K., Bottieau, J., Toubeau, J.-F., and Delarue, E. (2023). Strategic implicit balancing with energy storage systems via stochastic model predictive control. *IEEE Transactions on Energy Markets, Policy and Regulation*, 1:373–385.

TenneT (2022). Dutch market.

Topler, M. and Polajzer, B. (2020). Evaluation of the cross-border activation of the regulating reserve with dynamic simulations. *2022 IEEE International Conference on Environment and Electrical Engineering and 2022 IEEE Industrial and Commercial Power Systems Europe (EEEIC / ICPS Europe)*, c2 107:1–6.

van der Veen, R. A. C., Abbasy, A., and Hakvoort, R. (2010). Analysis of the impact of imbalance settlement design on market behaviour in electricity balancing markets.

van der Veen, R. A. C., Abbasy, A., and Hakvoort, R. A. (2011). Analysis of the impact of cross-border balancing arrangements for northern europe. *2022 18th International Conference on the European Energy Market (EEM)*, pages 653–658.

Weidlich, A. and Veit, D. (2008). Agent-based simulations for electricity market regulation advice: Procedures and an example. *Jahrbücher für Nationalökonomie und Statistik*, 228:149–172.

Wu, Z., Zhou, M., Li, G., Zhao, T., Zhang, Y., and Liu, X. (2020). Interaction between balancing market design and market behaviour of wind power producers in china. *Renewable and Sustainable Energy Reviews*, 132:110060.

Yamujala, S., Das, K., Koivisto, M. J., Gupta, M., and Kanellas, P. (2023). Requirements of future european balancing markets: insights into imbalance volumes and generation availability. *IET conference proceedings.*, 2023:282–288.